Optics Letters

Single frequency tunable UV laser at 308 nm based on all-fiberized master oscillator power amplifiers

Lei Pan,[1,*] Jihong Geng,[1] Thomas F. Hanisco,[2] and Shibin Jiang[1]

[1]Advalue Photonics Inc., 2700 E Bilby Rd., Tucson, AZ 85706, USA
[2]NASA Goddard Space Flight Center, 8800 Greenbelt Rd., Greenbelt, MD 20771, USA
*Corresponding author: lpan@advaluephotonics.com

Received 5 August 2022; revised 13 October 2022; accepted 15 October 2022; posted 18 October 2022; published 7 November 2022

A tunable narrow linewidth UV laser near 308 nm is necessary for highly sensitive hydroxyl (OH) radical measurement. We demonstrated a high-power fiber-based single frequency tunable pulsed UV laser at 308 nm. The UV output is generated from the sum frequency of a 515 nm fiber laser and a 768 nm fiber laser, which are harmonic generations from our proprietary high-peak-power silicate glass Yb- and Er-doped fiber amplifiers. A 3.50 W single frequency UV laser with 100.8 kHz pulse repetition rate, 3.6 ns pulse width, 34.7 μJ pulse energy, and 9.6 kW peak power has been achieved, which represents the first demonstration, to the best of our knowledge, of a high-power fiber-based 308 nm UV laser. With temperature control of the single frequency distributed feedback seed laser, the UV output is tunable for up to 792 GHz at 308 nm.

https://doi.org/10.1364/OL.472559

Compact, robust, and tunable single frequency lasers are highly desirable for many applications,, such as optical metrology and interferometry, optical data storage and communication, high-resolution laser spectroscopy, and LIDAR (light detection and ranging). Recently, the developments of single frequency lasers have mainly been near 1 μm, 1.55 μm, and 2 μm. A single frequency laser at the UV wavelength is not commonly available. The hydroxyl (OH) radical is the key oxidant in the global atmosphere. The determination of the concentration of OH is critical to the understanding of atmospheric photochemistry [1]. An UV laser is needed to probe the electronic transition of OH near 308 nm. Owing to its very low concentrations (~10^6 molecule cm^{-3}), high reactivity, and subsequent short lifetime [τ(OH): 0.01–1 s], the detection of tropospheric OH radicals is extremely challenging. The laser-induced fluorescence (LIF) technique has sufficient sensitivity and accuracy for OH measurements [2]. Currently, the most common laser sources for LIF are nanosecond frequency doubled dye lasers pumped by frequency doubled Nd:YAG or Nd:YLF lasers [3]. Such a laser system would be bulky, delicate, and expensive making it unsuitable for many field measurements. Recently, the integrated path differential absorption (IPDA) LIDAR technique has been demonstrated with high sensitivity [4]. In order to realize IPDA LIDAR for OH measurement, a high-power tunable narrow linewidth pulsed laser near 308 nm is needed. Tunable 308 nm UV lasers have been achieved with diode lasers based on frequency conversion; however, they are mostly continuous wave (CW) with low output power from nW to mW levels [5–7].

In this work, we present a fiber-based single frequency tunable UV laser at 308 nm for NASA's OH LIDAR applications. The UV output is generated from the sum frequency of a 515 nm fiber laser [8] and a 768 nm fiber laser [9], which are harmonic generations from proprietary silicate glass high-peak-power large mode field diameter (MFD) Yb- and Er-doped fiber amplifiers, respectively. A 3.50 W single-mode UV output has been achieved with 100.8 kHz pulse repetition rate and 3.6 ns pulse width, corresponding to a pulse energy of 34.7 μJ and a peak a power of 9.6 kW. With temperature control of the single frequency distributed feedback (DFB) seed laser, the UV output is tunable for up to 792 GHz at 308 nm.

A schematic diagram of the laser configuration is shown in Fig. 1. The laser system layout consists of three parts, which are defined by green, red, and purple dashed lines, respectively. The green labels a 1030 nm all-fiber single frequency master oscillator power amplifier (MOPA) and its second harmonic (SH) generation. The red marks the 1535 nm all-fiber single frequency MOPA and its SH generation. The purple represents 308 nm UV generation by the sum frequency of the two SH generations. The 1030 nm and 1535 nm seed lasers are modulated single frequency DFB lasers with a pulse width of ~6 ns and a pulse repetition rate of 100.8 kHz. Both seed lasers have a linewidth of a few GHz; there is a frequency chirp induced by direct modulation of the DFB lasers. A narrower linewidth can be obtained by generating pulses with external modulation. The two DFB lasers are trigged and synchronized by a function generator. For the 1030 nm seed laser, multi-stage Yb fiber pre-amplifiers are employed to increase the seed power to ~100 mW before it is sent to the main Yb fiber amplifier. Considering the relatively lower gain of the Er-doped main fiber amplifier, the 1535 nm seed laser was boosted to ~1.0 W by multi-stage Er fiber pre-amplifiers.

The main fiber amplifiers are fabricated with Advalue Photonics proprietary highly (Yb or Er)-doped silicate glass fibers. The large MFD (Yb ~40 μm and Er ~50 μm; both numerical apertures < 0.04) and short fiber length (Yb ~20 cm, 976 nm residual pump ~10%; Er ~30 cm, 976 nm residual pump ~50%) enable the amplifiers to generate up to a few hundred μJ nanosecond pulses without showing any stimulated Brillouin scattering (SBS) effects. The seed laser and 976 nm pump laser are coupled

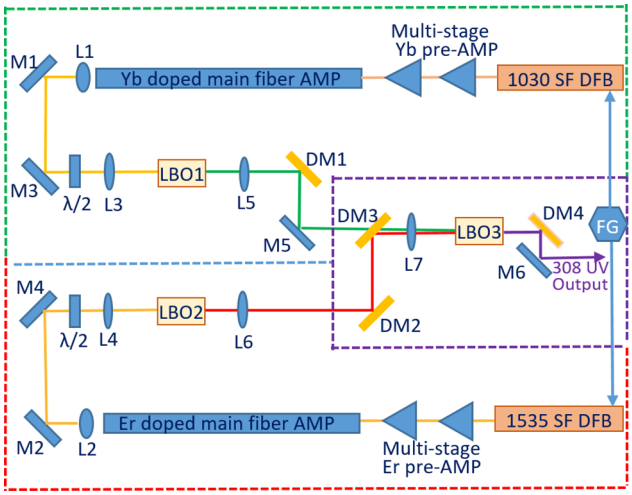

Fig. 1. Schematic diagram of the experimental setup. M: high reflection mirror, DM: dichroic mirror, L: lens, AMP: amplifier, SF DFB: single frequency distributed feedback laser, λ/2: half-wave plate; LBO: lithium triborate crystal, FG: function generator.

to the main amplifier by a $(2+1)\times 1$ pump combiner. A fiberized mode adaptor is fabricated before the gain fiber to ensure highly efficient seed laser coupling without exciting higher order modes. Both 1030 nm and 1535 nm MOPAs are all polarization maintaining (PM) fiber splicing and their outputs are linearly polarized, which are ready for the SH generation.

The high-power IR outputs from the main fiber amplifiers are collimated (L1 and L2) and focused (L3 and L4) to nonlinear crystals (LBO1 and LBO2) with non-critical phase matching (NCPM) for SH generation (515 nm and 768 nm). Then, the 515 nm and 768 nm lasers are collimated (L5 and L6), combined (DM3), and then focused (L7) to another LBO crystal (LBO3) for frequency mixing. The LBO3 crystal has dimensions of 3mm × 3mm × 35 mm with an input surface anti-reflection (AR) coated at 515 nm and 768 nm and output surface AR coated at 308 nm. The crystal is cut for critical phase matching (CPM: θ = 90°, Φ = 56°). The residual 515 nm and 768 nm lasers after LBO3 are dumped by a dichroic mirror DM4 and the 308 nm UV light is outputted by M6.

The performance of the 1030 nm main fiber amplifier and its SH generation are depicted in Fig. 2. At a pump power of 42.0 W, the 1030 nm IR output power is 18.8 W, corresponding to a slope efficiency of 55.0%. With a NCPM LBO crystal, 11.9 W 515 nm green output power is obtained, corresponding to a SH conversion efficiency of 63.3%. Figure 3(a) shows the measured green laser pulse shape with a pulse width of 6.3 ns. The calculated SH pulse energy is 118 μJ and the peak power is 18.7 kW. The green laser beam profile measured by an Ophir Nanoscan at the L7 position is shown in Fig. 3(b). It is a perfect single mode with excellent beam roundness of ~99%. The beam diameter in the x and y directions is $d_x = 1.14$ mm and $d_y = 1.15$ mm, respectively.

The wavelength tuning is realized by thermoelectric cooler (TEC) temperature control of the 1030 nm DFB seed laser. From 15.0 to 35.0°C, the wavelength is tuned from 1028.7 nm to 1030.1 nm, as shown in Fig. 4. The total wavelength tuning range is $\Delta\lambda_{1030} = 1.40$ nm (70 pm/°C), which corresponds to $\Delta\lambda_{515} = 0.70$ nm (35 pm/°C) and $\Delta\lambda_{308} = 0.25$ nm (12.5 pm/°C), respectively. In the frequency domain, the tuning range is

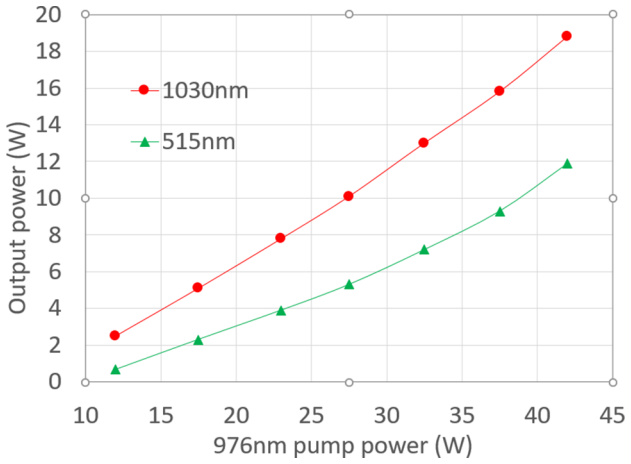

Fig. 2. Yb-doped main fiber amplifier output and its SH generation: 1030 nm and 515 nm output versus 976 nm pump power.

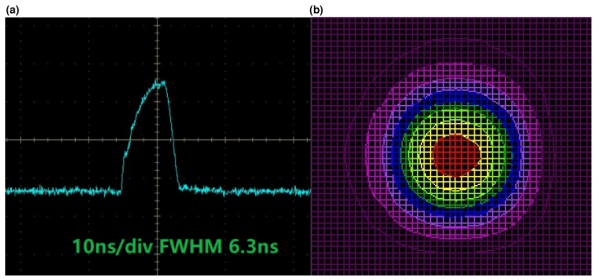

Fig. 3. (a) 515 nm laser pulse shape; (b) 515 nm laser beam profile. Both are measured at 11.9 W output.

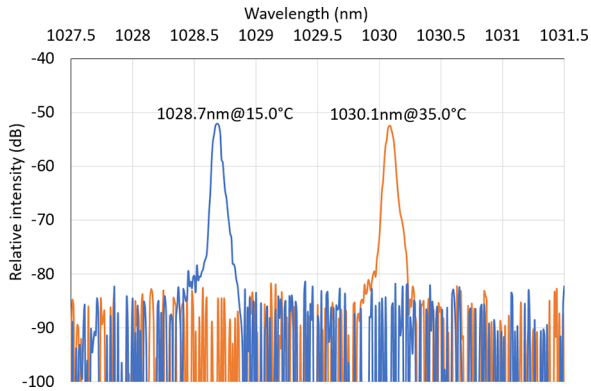

Fig. 4. 1030 nm DFB seed laser wavelength tuning by TEC temperature control; the optical spectrum analyzer (OSA) resolution is 0.06 nm.

~396 GHz @1030 nm and ~792GHz@ 515 nm and 308 nm. To keep the phase matching and the SH power constant during wavelength tuning, the temperature of the LBO1 crystal should be decreased from ~194.1 to ~192.3°C, accordingly.

For the 1535 nm main fiber amplifier, Er-only doped fiber has much lower absorption at 976 nm than Yb-doped fiber. In addition, the gain fiber length is limited by the laser footprint size and SBS threshold. Therefore, its slope efficiency is much lower than that of the 1030 nm main fiber amplifier. At a pump power of 135 W, the 1535 nm IR output power is 11.0 W, corresponding

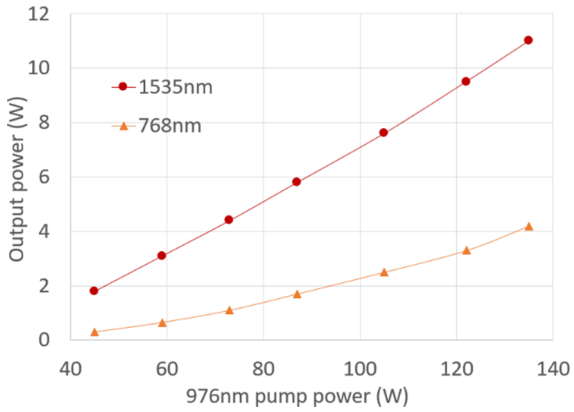

Fig. 5. Er-doped main fiber amplifier output and its SH generation: 1535 nm and 768 nm output versus 976 nm pump power.

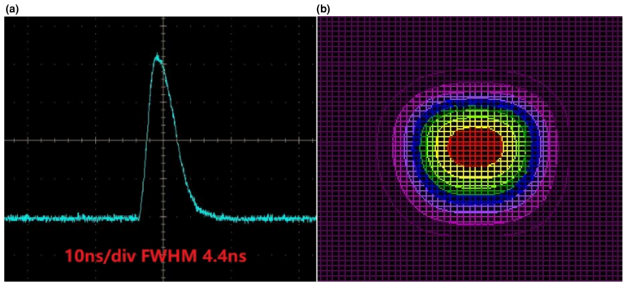

Fig. 6. (a) 768 nm laser pulse shape; (b) 768 nm laser beam profile. Both are measured at 4.2 W output.

to a slope efficiency of 10.2%, as shown in Fig. 5. With a NCPM LBO crystal and a temperature setting of ~110°C, 4.2 W 768 nm output power is obtained, corresponding to a SH conversion efficiency of 38.2%. The 1535 nm pulse peak power is not high enough to achieve a highly efficient SH generation. In addition, the center peak of the pulse has higher SH efficiency than the edge. Therefore, the 768 nm pulse becomes even shorter (4.4 ns versus 6 ns) than the 1535 nm pulse, as shown in Fig. 6(a). The calculated pulse energy is 41.7 μJ and peak power is 9.5 kW. The 768 nm laser beam profile measured at the L7 position by the Ophir Nanoscan is shown in Fig. 6(b). It is a single mode with a slight beam ellipticity of ~85%. The ellipticity is believed to have originating from the beam profile of the 1535 nm main fiber amplifier output. The beam diameter in the x and y directions is $d_x = 1.65$ mm and $d_y = 1.41$ mm, respectively.

To achieve an efficient sum frequency conversion, the two SH laser pulses must be well overlapped both in time and in space. The temporal overlap is realized by adjusting the delay of the function generator. The spatial overlap could be optimized by the mirrors, such as DM2, DM3, and M5. Since the 1030 nm MOPA and its SH generation have much higher efficiencies than the 1535 nm MOPA and its SH, to make the best use of the 768 nm laser power in frequency conversion, the 515 nm green laser has been set to run at relatively high output levels: 7.2 W, 9.3 W, and 11.9 W. The 308 nm outputs versus 768 nm inputs at different 515 nm input power levels are shown in Fig. 7. With the 11.9 W 515 nm laser and the 4.2 W 768 nm laser, a maximum of 3.50 W 308 nm UV output has been generated, corresponding to an UV laser pulse energy of 34.7 μJ.

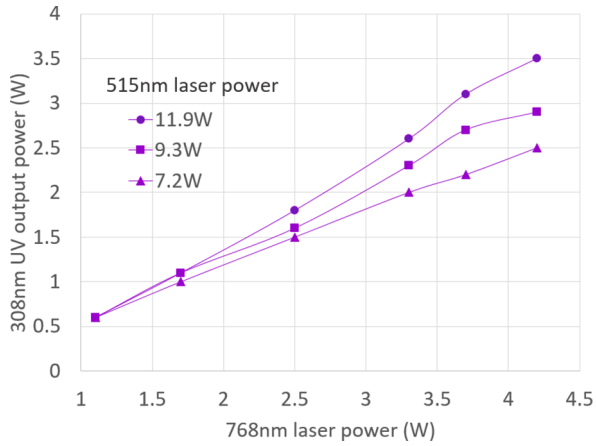

Fig. 7. 308 nm output versus 768 nm input at different 515 nm input power levels.

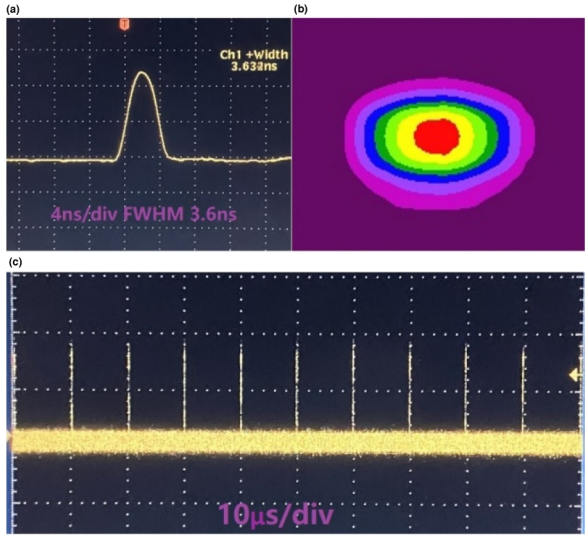

Fig. 8. 308 nm UV output measurement at 3.50 W output power: (a) pulse shape with 3.6 ns pulse width; (b) beam profile measured by an Ophir Nanoscan; (c) pulse train with pulse repletion rate of 100.8 kHz.

The UV laser pulses are measured by a fast Si photodetector. As shown in Fig. 8(a), the 308 nm UV laser pulse width is 3.6 ns and the calculated peak power is 9.6 kW. The measured UV laser pulse train is shown in Fig. 8(c). It operates at a 100.8 kHz repetition rate with very low pulse intensity fluctuations. Figure 8(b) shows the 308 nm UV laser beam profile measured by the Ophir Nanoscan. It is a nice single mode with a beam ellipticity of ~68%. The ellipticity is due to the spatial walk-off effects in the nonlinear conversion, since the LBO crystal used here is pretty long (35 mm). The laser output spectrum measured by a StellarNet bluewave compact USB spectrometer is shown in Fig. 9. Besides 308 nm UV light, the spectrometer has been intentionally tilted to collect a tiny residual of the 515 nm and 768 nm lasers, which is dumped behind DM4. Therefore, all three wavelengths involved in the sum frequency are shown in the spectrum measurement. The laser has been delivered and installed in NASA Goddard Space Flight Center (GSFC) for

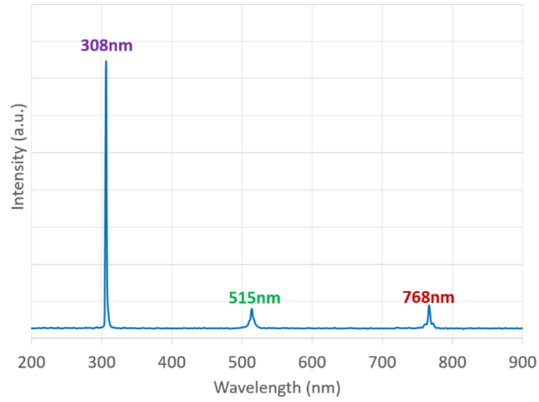

Fig. 9. Laser spectrum measured by a StellarNet bluewave compact USB spectrometer.

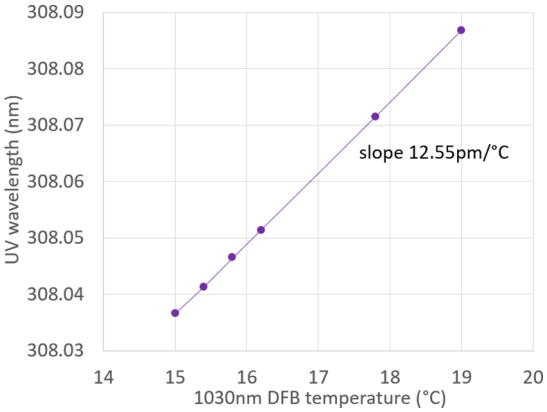

Fig. 10. UV wavelength tuning measurement for 1030 nm DFB temperature from 15.0 to 19.0°C.

the OH LIDAR project. Figure 10 shows the 308 nm UV wavelength tuning measurement performed at the NASA GSFC lab. For the 1030 nm DFB temperature from 15.0 to 19.0°C, the UV wavelength increases from 308.0366 nm to 308.0868 nm, corresponding to a tuning rate of 12.55 pm/°C, which agrees well with the prediction by the 1030 nm wavelength tuning described in Fig. 4.

In summary, with high-peak-power silicate glass Yb- and Er-doped fiber amplifiers and frequency conversion, we demonstrated a fiber-based single frequency tunable UV laser at 308 nm for OH LIDAR applications. A 3.50 W single-mode 308 nm UV output has been achieved with a wavelength tuning capability of up to 792 GHz. Since both Yb- and Er-doped fibers have broad gain spectra and wide wavelength tuning range of up to 100 nm [10,11], this technology could be potentially extended to other UV wavelengths and meet more applications.

Funding. Goddard Space Flight Center (80NSSC19C0145).

Disclosures. The authors declare no conflicts of interest.

Data availability. Data underlying the results presented in this paper are not publicly available at this time but may be obtained from the authors upon reasonable request.

REFERENCES

1. C. N. Hewitt and R. M. Harrison, Atmos. Environ. **19**, 545 (1985).
2. F. Holland, M. Hessling, and A. Hofzumahaus, J. Atmos. Sci. **52**, 3393 (1995).
3. M. Strotkamp, A. Munk, B. Jungbluth, K. Dahlhoff, P. Jansen, S. Broch, S. Gomm, M. Bachner, H. Fuchs, F. Holland, and A. Hofzumahaus, Proc. SPIE **8599**, 85990L (2013).
4. H. Riris, K. Numata, S. Li, S. Wu, A. Ramanathan, M. Dawsey, J. Mao, R. Kawa, and J. B. Abshire, Appl. Opt. **51**, 8296 (2012).
5. D. B. Oh, Opt. Lett. **20**, 100 (1995).
6. L. Corner, J. S. Gibb, G. Hancock, A. Hutchinson, V. L. Kasyutich, R. Peverall, and G. A. D. Ritchie, Appl. Phys. B **74**, 441 (2002).
7. M. Büki, D. Röser, and S. Stellmer, Appl. Opt. **60**, 9915 (2021).
8. Advalue Photonics Inc. EVERESTnano Green Pulsed Laser https://www.advaluephotonics.com/products/everestnano-green-pulsed-laser-ap-515
9. W. Lee, J. Geng, Z. Qiang, L. Pan, S. Jiang, F. S. Anderson, X. Mu, and S. M. Beck, IEEE Photonics Technol. Lett. **31**, 1534 (2019).
10. J. Hu, L. Zhang, and Y. Feng, in *Advanced Solid State Lasers (ASSL)*, (Optica Publishing Group, 2014), paper AM5A.22.
11. X. Dong, N. Q. Ngo, P. Shum, H.-Y. Tam, and X. Dong, Opt. Express **11**, 1689 (2003).